Proceedings of the ASME 2010 3rd Joint US-European Fluids Engineering Summer Meeting and 8th International Conference on Nanochannels, Microchannels, and Minichannels
FEDSM-ICNMM2010
August 1-5, 2010, Montreal, Canada

FEDSM-ICNMM2010-30812

BUCKLING OF HUMAN AORTA RELATED TO DISSECTION DUE TO FLOW-PRESSURE CONDITIONS

Kostas Karagiozis
Department of Mechanical Engineering
McGill University
817 Sherbrooke Street West
Montreal, Quebec, Canada, H3A 2K6
konstantinos.karagiozis@mcgill.ca

Marco Amabili
Department of Mechanical Engineering
McGill University
817 Sherbrooke Street West
Montreal, Quebec, Canada, H3A 2K6
marco.amabili@mcgill.ca

Rosaire Mongrain
Department of Mechanical Engineering
McGill University
817 Sherbrooke Street West
Montreal, Quebec, Canada, H3A 2K6
rosaire.mongrain@mcgill.ca

Raymond Cartier
Montreal Heart Institute Research Centre
5000, Bélanger Street
Montreal, Quebec, Canada, H1T 1C8
rc2910@aol.com

Michael P. Païdoussis
Department of Mechanical Engineering
McGill University
817 Sherbrooke Street West
Montreal, Quebec, Canada, H3A 2K6
mary.fiorilli@mcgill.ca

ABSTRACT

Human aortas are subjected to large mechanical stresses and loads due to blood flow pressurization and through contact with the surrounding tissue and muscle. It is essential that the aorta does not lose stability for proper functioning. The present work investigates the buckling of human aorta relating it to dissection by means of an analytical model. A full bifurcation analysis is used employing a nonlinear model to investigate the nonlinear stability of the aorta conveying blood flow. The artery is modeled as a shell by means of Donnell's nonlinear shell theory retaining in-plane inertia, while the fluid is modelled by a Newtonian inviscid flow theory but taking into account viscous stresses via the time-averaged Navier-Stokes equation. The three shell displacements are expanded using trigonometric series that satisfy the boundary conditions exactly. A parametric study is undertaken to determine the effect of aorta length, thickness, Young's modulus, and transmural pressure on the nonlinear stability of the aorta. As a first attempt to study dissection, a quasi-steady approach is taken, in which the flow is not pulsatile but steady. The effect of increasing flow velocity is studied, particularly where the system loses stability, exhibiting static collapse. Regions of large mechanical stresses on the artery surface are identified for collapsed arteries indicating possible ways for dissection to be initiated.

1. INTRODUCTION

The mechanisms leading to static collapse and flutter of arteries, veins and pulmonary passages may be said to be well understood, though the means of prediction are not yet fully satisfactorily explained, mainly because of the large deformations involved. Nevertheless, there are numerous studies on the collapse and flutter of collapsible tubes modelling blood flow in veins, pulmonary passages and the urethra; see for example the reviews by Kamm & Pedley [1], Bertram [2] and Païdoussis [3]; and the papers by Luo and Pedley [4], and Heil [5,6], for instance.

Furthermore, with the introduction of classical bifurcation theory in applied mechanics, advanced mathematical models were conceptualized producing new theoretical findings for the nonlinear response of shells under external loading. It is important to distinguish the notion of word the "bifurcation" used as a mathematical concept to the use in the medical community. In general, bifurcation in medical science is associated with the split of an artery (or a vein) and the generation of new arterial branches. However, in the mathematical interpretation, bifurcation signals the qualitative change of a solution and the generation of new solution branches that describe new dynamical behaviour of the system [7, 8]. A significant advantage of using bifurcation analysis compared to a finite element analysis is that bifurcation theory identifies all possible stable and unstable solutions of the system for a range of the critical parameter of the system (i.e., flow velocity or the transmural pressure in the present analysis) *vis-á-vis* results obtained from finite element analysis (FEA) models which tend to produce results for only a specific value of the critical parameter. In a series of benchmark theoretical papers Amabili et al. [9-12] used bifurcation theory to analyze simply supported shells subjected to external force or fluid flow. It was found that the shells lose stability by divergence, exhibiting a strong subcritical behavior. These findings were confirmed by experiments for clamped shells [13].

One of the most catastrophic cardiovascular diseases is associated with the dissection of the upper aorta by a sudden rupture of the internal layer of the aortic wall [14]. It is assumed that the mechanical stresses applied on the aorta wall, due to specific pressure-flow conditions, exceed some critical value, resulting in local rupture of the artery tissue that propagates in the axial direction following a helicoidal path in the inner two-thirds and outer one-third of the media [15, 16]. According to recent studies, the prevalence of the aortic wall dissection occurs for 2.6-3.5 per 100,000 person-years, with a mortality increase of up to 2% per hour after symptoms have been detected [17, 18]. Even though the general assumption is that high mechanical stresses causing inner tissue rupture in the aorta are a significant factor for the total rupture of aorta, the underlying mechanism of aorta dissection is poorly understood. The main reason that the rupture mechanism has not yet been clearly determined is that direct measurements of the risk factors *in vivo* are not feasible [19]. The aorta is a complex part of the circulation system, changing dramatically in shape and size according to the systolic and diastolic pressure field, as well as in material properties due to mechanical stresses and age; accordingly, simulation of aortic dynamics is extremely difficult [20].

The present paper proposes to study aortic dissection by means of an analytical model – thus following in the path of Heil's [5] and Heil & Pedley's [21] studies. The artery is modelled as a shell by means of Donnell's nonlinear shell theory, while the fluid is modelled by a Newtonian inviscid flow theory but taking into account viscous stresses via the time-averaged Navier-Stokes equations. As a first attempt to describe the nonlinear behaviour of the aorta, a quasi-steady approach is taken, in which the flow is not pulsatile but steady. The effect of increasing flow velocity is studied, particularly in the neighbourhood of the system losing stability by static divergence. Bifurcation theory is used to analyze the system of equations of motion for the aortic wall.

2. THEORY

The model of the aortic segment consists of a circular cylindrical shell of length L, mean radius R, and thickness h, such that $h/R \ll 1$, shown in Fig.1. The origin of the cylindrical coordinate system, $(O;\, x, r, \theta)$, is positioned at the center of one end of the shell. The shell is assumed to be of homogeneous, isotropic elastic material of Young's modulus E and Poisson ratio ν [22]. The displacements of the shell middle surface are denoted by u, v and w, in the axial, circumferential and radial directions, respectively; w is taken positive outward. The mathematical details are given in [23].

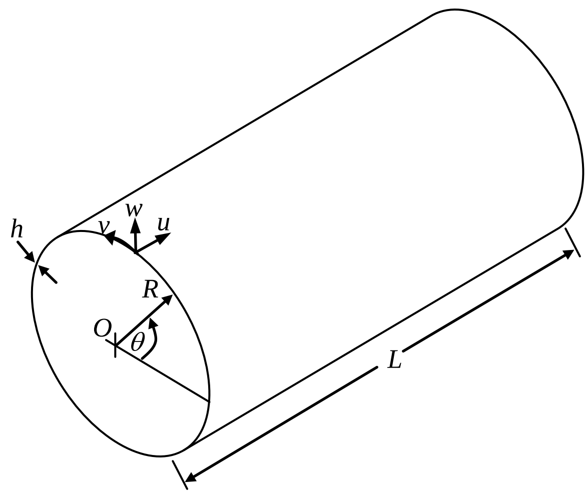

FIGURE 1: The configuration of the cylindrical shell section used to simulate the ascending aortic segment.

The nonlinear Donnell equations for a shell were used to describe the shell motion [24],

$$\mathbf{M}\begin{Bmatrix}\ddot{u}\\ \ddot{v}\\ \ddot{w}\end{Bmatrix}+\mathbf{C}\begin{Bmatrix}\dot{u}\\ \dot{v}\\ \dot{w}\end{Bmatrix}+\left[\mathbf{K}+\mathbf{N_2}\begin{Bmatrix}u\\ v\\ w\end{Bmatrix}+\mathbf{N_3}\left(\begin{Bmatrix}u\\ v\\ w\end{Bmatrix},\begin{Bmatrix}u\\ v\\ w\end{Bmatrix}\right)\right]\begin{Bmatrix}u\\ v\\ w\end{Bmatrix}=\begin{Bmatrix}0\\ 0\\ \Delta P_{\mathrm{tm}}\end{Bmatrix};\quad (1)$$

here **M** is the mass matrix (including the effect of the fluid), **C** the damping matrix, **K** the linear stiffness matrix which does not include the displacement effects, $\mathbf{N_2}$ a matrix that gives the quadratic nonlinear terms for the displacements, $\mathbf{N_3}$ a matrix that involves the cubic nonlinear terms for the displacements, and ΔP_{tm} the transmural pressure on the artery in the radial direction.

The following boundary conditions are imposed at the shell ends:

$$v = w = w_0 = 0, \qquad \text{at } x = 0, L, \qquad (2a\text{-}c)$$

$$N_x = -k_a\, u \qquad \text{at } x = 0, L, \qquad (2d)$$

$$M_x = -k_r\, (\partial w/\partial x), \qquad \text{at } x = 0, L, \qquad (2e)$$

where N_x is the axial stress resultant per unit length, M_x the bending moment per unit length, k_a and k_r are stiffness per unit length of the axial and rotational constraints, respectively.

A base of shell displacements is used to discretize the system; the displacements u, v and w can be expanded by using the following expressions, which identically satisfy boundary conditions (2a,b):

$$u(x,\theta,t)=\sum_{m=1}^{5}\left[u_{m,n,c}(t)\cos(n\theta)+u_{m,n,s}(t)\sin(n\theta)\right]\cos(\lambda_m x)$$

$$+\sum_{m=1}^{3}u_{m,2n,c}(t)\cos(2n\theta)\cos(\lambda_m x)+\sum_{m=1}^{4}u_{2m-1,0}(t)\cos(\lambda_{2m-1}x), \tag{3a}$$

$$v(x,\theta,t)=\sum_{m=1}^{5}\left[v_{m,n,c}(t)\sin(n\theta)+v_{m,j,s}(t)\cos(n\theta)\right]\sin(\lambda_m x)$$

$$+\sum_{m=1}^{4}v_{m,2n,c}(t)\sin(2n\theta)\sin(\lambda_m x), \tag{3b}$$

$$w(x,\theta,t)=\sum_{m=1}^{3}\left[w_{m,n,c}(t)\cos(n\theta)+w_{m,n,s}(t)\sin(n\theta)\right]\sin(\lambda_m x)$$

$$+\sum_{m=1}^{4}w_{2m-1,0}(t)\sin(\lambda_{2m-1}x), \tag{3c}$$

where n is the number of circumferential waves, m is the number of longitudinal half-waves, $\lambda_m=m\pi/L$, and t is the time; $u_{m,j}(t)$, $v_{m,j}(t)$ and $w_{m,j}(t)$ are the generalized coordinates, which are unknown functions of t; the additional subscript c or s indicates if the generalized coordinate is associated to a driven mode (i.e. a mode directly excited by the external excitation) or a companion mode (i.e. a mode not directly excited and contributing to the system response due to nonlinear coupling); no additional subscript is used for axisymmetric terms. The total number of degrees of freedom used in the present model is 42.

The kinetic energy of the shell is given by

$$T_S=\frac{1}{2}\rho_S h\int_0^{2\pi}\int_0^{L}\left(\dot{u}^2+\dot{v}^2+\dot{w}^2\right)\mathrm{d}x\,R\,\mathrm{d}\theta, \tag{4}$$

where ρ_S is the mass density of the shell. The potential energy of the shell U_S is made up of two contributions: the elastic strain energy U_{shell} of the circular cylindrical shell and the potential energy U_{spring} stored by the axial and rotational distributed springs at the shell ends; therefore,

$$U_S=U_{\text{shell}}+U_{\text{spring}}. \tag{5}$$

The elastic strain energy U_{shell} of a circular cylindrical shell is given by [24]

$$U_{\text{shell}}=\frac{1}{2}\int_0^{2\pi}\int_0^{L}\int_{-h/2}^{h/2}\left(\sigma_x\varepsilon_x+\sigma_\theta\varepsilon_\theta+\tau_{x\theta}\gamma_{x\theta}\right)\mathrm{d}x\,R(1+z/R)\,\mathrm{d}\theta\,\mathrm{d}z, \tag{6}$$

where the stresses σ_x, σ_θ and $\tau_{x\theta}$ are related to the strains ε_x, ε_θ and $\varepsilon_{x\theta}$ for homogeneous isotropic material ($\sigma_z=0$, case of plane stress). Donnell's nonlinear shell theory [24] retaining in-plane inertia is used in order to evaluate equations (4)-(6). The model has been developed and validated in [23].

The potential energy stored by the axial and rotational springs at the shell ends is given by

$$U_{\text{spring}}=\frac{1}{2}\int_0^{2\pi}\left\{k_a\left[(u_a)_{x=0}\right]^2+k_a\left[(u_a)_{x=L}\right]^2+k_r\left[\left(\frac{\partial w}{\partial x}\right)_{x=0}\right]^2\right.$$

$$\left.+k_r\left[\left(\frac{\partial w}{\partial x}\right)_{x=L}\right]^2\right\}\mathrm{d}\theta, \tag{6}$$

where u_a is the axial displacement given by equation (3a) without the axisymmetric terms $u_{m,0}(t)$.

2.1 Fluid model

The shell is assumed to be positioned within a large concentric solid tube filled with quiescent fluid to include the effect of the inertia of the fluid surrounding the aorta. The contained flowing fluid and the external quiescent fluid are assumed to be incompressible and inviscid and the flow isentropic and irrotational, so that potential theory can be used to describe fluid motion. Nonlinear effects in the dynamic pressure and in the boundary conditions at the fluid-structure interface are negligible [25]. The shell prestress due to the fluid weight is also neglected. The fluid motion is described by the velocity potential Φ, which satisfies the Laplace equation. A very long shell periodically supported at distance L is assumed in order to use the separation of variables method. The fluid model is based on the mathematical formulation given in Païdoussis and Denise [26] and later elaborated by [9].

The irrotationality property is the condition for existence of a scalar potential function Ψ, from which the velocity may be written as

$$\mathbf{v}=\nabla\Psi. \tag{7}$$

By using the Green's theorem, the total energy E_F associated with the flow can conveniently be divided into three terms with different contributions of time functions and their derivatives:

$$E_F=T_F+E_G-V_F; \tag{8}$$

the first and second of the three terms on the right-hand side can be identified as the kinetic and gyroscopic energies, respectively; an opposite sign is introduced for the potential energy V_F, for convenience.

The time-mean Navier-Stokes equations are employed to calculate the steady viscous effects assuming that the flow is fully turbulent [23, 27]. This type of hybrid model is particularly efficient from the computational point of view.

The final Lagrange equations of motion maybe written as:

$$\frac{\mathrm{d}}{\mathrm{d}t}\left[\frac{\partial(T_S+T_F)}{\partial\dot{q}_j}\right]-2\frac{\partial E_G}{\partial q_j}+\frac{\partial(U_S+V_F)}{\partial q_j}=Q_j,\ j=1,\dots,N_{\mathrm{T}}, \tag{9}$$

where T_S and T_F are the kinetic energy of the shell and the fluid, respectively, U_S and V_F are the potential energy of the shell and the fluid, respectively, E_G is the gyroscopic energy, and Q_j are the generalized external forces, including the transmural pressure ΔP_{tm} and damping.

The resulting forty-two, second-order nonlinear ordinary differential equations are divided by the modal mass and further simplified to first-order differential equations. Once nondimensionalized, the resulting ODEs are studied via a continuation method to perform a full bifurcation analysis. The software AUTO employs the pseudo-arclength continuation and collocation methods for continuation of the solution, bifurcation analysis and branch switching [28].

3. NUMERICAL RESULTS

The aorta wall is simulated by a single-layered shell with specified thickness ranging from $h = 7\times10^{-4}$ m to 1.5×10^{-3} m [29, 30]. The average diameter of the aorta is between 20 and 30 mm [31]. The length of the simulated aorta ranged from 0.126 to 0.40 m. In most of the simulations an average shell radius of R=0.01575 m was used along with different length-to-radius ratios L/R ~ 8, 12, 19, and 25, However, additional results were obtained also for R/h= 10.5 and 22.5.

The value of Young's modulus was assumed to take the following values, representing different material stiffnesses corresponding to different pathological cases that affect the rigidity of the aortic wall [22, 32]: 100, 400 and 800 kPa. The mass density of aorta was assumed to be 1200 kg/m^3 and the Poisson's ratio was set to ν=0.49 [22].

The fluid in our analysis is considered Newtonian with a density of 1050 kg/m^3 and a kinematic viscosity of 4×10^{-6} m^2/s (4 centi-stokes). A Newtonian approximation has been considered to be acceptable for calculations related to large arteries like the aorta [32, 33, 34]. In addition, the flow is considered to be fully turbulent which is a valid assumption for the straight cylindrical shell at sufficiently high flow velocities (for these simulations, the range of interest of the Reynolds number is 4×10^3-7×10^3 for which a fully developed turbulent velocity profile is expected). The roughness of the arterial wall used in the Colebrook equation was set equal to 2×10^{-5} m which corresponds to the thickness of the endothelial cells lining the wall [35, 36].

The flexible boundary conditions at the shell ends were assumed to simulate relatively stiff axial and radial constraints not allowing for any displacements but allowing rotations. The axial and radial spring constraints were set to k_{a1}= 1×10^7 N/m^2, k_{a2}= 1×10^5 N/m^2 and k_r= 0 N/rad. The critical circumferential wavenumber at the onset of instability was found to be n=2 in all simulations. The value of the transmural pressure ΔP_{tm} simulated different pressure loadings ranging from 0 Pa to 4 kPa (typical values observed in the lower abdominal aorta). In the present model both the flow and the pressure are assumed to be constant, although it is well known that they are both periodic functions with a phase delay between them [37]. Here it is assumed that instability could be triggered by an unfavourable combination of these two parameters, irrespective of pulsation, which is a reasonable assumption. It is important to mention that in the numerical calculations the aorta was assumed to be confined within a larger solid cylinder with a diameter equal to ten times the diameter of the aorta. Therefore, the effect of the inertia of the fluid surrounding the aorta was also taken into consideration in the numerical experiments. A non-dimensional fluid velocity $V = U\Big/\left\{\left(\pi^2/L\right)\left[D/\left(\rho h\right)\right]^{1/2}\right\}$ is introduced for convenience, defined as in [38], where U is the dimensional flow velocity and $D = E h^3/[12(1-\nu^2)]$. A damping ratio $\zeta_{1,2}$ = 0.012 is taken into account in all the calculations. All calculations were performed with a kinematic viscosity of 3.5×10^{-5} m^2/s and aorta inner surface roughness of 0.0686. Additional results for a critical circumferential wavenumber n=3 revealed similar trends as for n=2.

3.1 Collapse of aortic segment conveying blood

For this numerical experiment, R/h=22.5 was taken, simulating a thin aorta. Table 1 summarizes the geometry and material properties used in this simulation.

Geometry			Structure			Fluid
L(m)	R (m)	h (m)	E (Pa)	ν	ρ_s(kg/m^3)	ρ_f(kg/m^3)
0.126	0.01575	0.0007	800000	0.49	1200	1050

Table 1: System properties for an aorta conveying blood with n=2. L is the length of the aorta, R the mean radius, h the thickness, E the Young's modulus, ν the Poisson ratio, ρ_s the density of the aorta, and ρ_f the density of the flowing fluid.

The flow velocity was increased gradually from 0 to 2.1 m/s with ΔP_{tm}=0. Figure 2 shows the resulting bifurcation diagram as a plot of the (maximum radial deformation)/h versus the flow velocity for mode n=2, m=1 (two circumferential waves and half axial wave), denoted as $w_{1,2}$.

The results in Fig.2 display the nonlinear behaviour of an aorta conveying blood. The deformation follows solution branch 1 with zero amplitude (meaning that the aorta maintained its original circular shape). However, when the blood flow velocity reaches 1.55 m/s the system loses stability by static divergence (this is the point of the linear onset of instability), generating the new solution branches 2. Divergence (buckling) in this case means that a new static solution emerged with a distinctive circumferential wavenumber of n=2 (the aorta wall moved inwards creating two lobes, thus n=2). Solution branch 2 is initially unstable (dotted lines), the locus moving to the left. It is stabilized for a small range of flow velocities from 0.5297 to 0.5354 m/s. The solution then remains unstable until it reaches the folding points at U=0.5063 m/s, whereupon branch 2 folds and becomes stable, increasing its amplitude with increasing flow velocity.

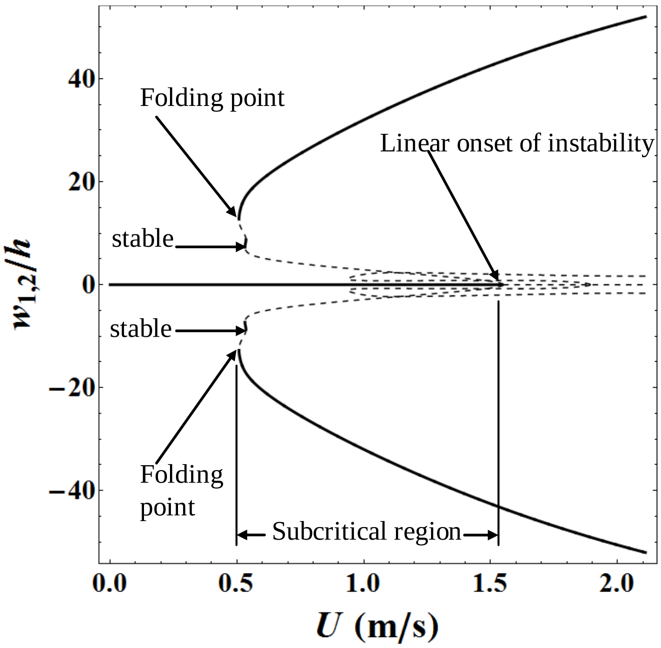

FIGURE 2: Bifurcation diagram of dimensional flow velocity versus nondimensional radial displacement for the first asymmetric mode. ——— Stable solutions; - - - - - unstable solutions.

These results indicate that an aorta may lose stability by divergence and exhibit a highly subcritical nonlinear behaviour, such that there is a large range of flow velocities in which multiple stable aorta configurations coexist for the specific flow and pressure conditions. This result means that, in this flow range ($0.5063<U<1.55$ m/s) – the subcritical range – the aorta may *jump* from one stable configuration to another (and *vice versa*), if enough perturbation is given to the system in the form of a flow spike, transmural pressure perturbation or external force (trauma case); this clearly results in increased mechanical stresses on the aortic wall. This also means that a *catastrophic* failure may occur (aorta wall collapses with deformation that is large enough for inner-wall contact and complete folding or kinking of the aorta). This in turn may cause significant material damage (aorta wall dilation) in pathological situations, weakening transverse aorta wall stiffness and perhaps leading to the initiation of aneurysm or dissection (delamination of the wall layers).

As the blood flow velocity increases or decreases in the diastolic-systolic cycle, it is evident that the deformation of the aorta may follow any of the stable branches, increasing or decreasing the mechanical stresses acting on the aortic wall, making it prone to failure due to microscopic fatigue [39].

The result shown in Fig.2 is a simplified two-dimensional representation of the actual aorta behaviour. In fact, the buckling could occur in any direction due to the axial symmetry of the system. Once buckling has been initiated at a specific angle θ, it propagates (i.e. increases in amplitude) as the flow velocity increases following a helicoidal path [9]. The solution branches shown in Fig. 2 represent the generatrix of the axisymmetric surface on which the helicoidal path. Interestingly, these results are in qualitative agreement with clinical observations regarding the propagation of dissection in human aortas [40].

Figure 3 shows a graphical interpretation of the aorta deformation for different blood flow velocities within the subcritical flow range (here all the modes were considered when computing the total displacement w in the radial direction). It is evident that at the neighbourhood of maximum deflection large stresses are generated due to the high curvature, which could lead to dissection [41].

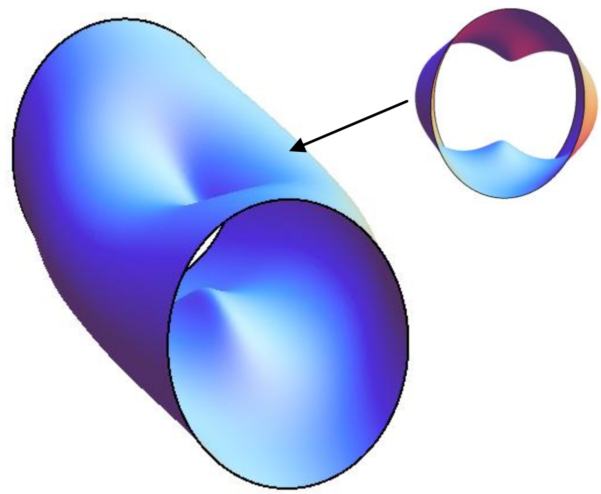

FIGURE 3: Deformation of the aortic wall segment for U=0.531 m/s indicating regions of high stress at midlegth.

3.2 Nonlinear response of aorta for different *L*/*R* ratios

The boundary conditions at the shell ends for these cases were set to allow for axial and circumferential displacements at the aorta ends ($k_{a1}= k_{a2}= 0$ N/m^2 and $k_r= 0$ N/rad). These calculations were performed for E=100 kPa, n=2, and zero transmural pressure.

The results, shown in the bifurcation diagram in Fig. 4, indicate that the critical flow velocity for the onset of instability (linear limit) decreases as expected with increasing the length of the aorta. It actually decreases in half if the aorta length triples in length. Nevertheless, the effect of *L*/*R* ratio on the re-stabilization velocity (folding point) is even more augmented with increasing the *L*/*R* ratio. In fact, the change on the folding velocity value is 2.5 times smaller for a length three times larger. The frequency is also reduced with increasing the length of aorta.

The aorta in all cases lost stability by divergence, generating two unstable solutions (branches denoted by number 2) that become stable after folding. This subcritical behaviour generates regions of multiple stable solutions at blood flow velocities much smaller than the one predicted by linear theory. It is also evident that for longer aortas the subcritical behaviour is more profound and the solution branches 2 become stable (after folding) with much higher deformation amplitudes (in some cases critical inner wall contact might occur right after folding) than in cases with shorter aortas.

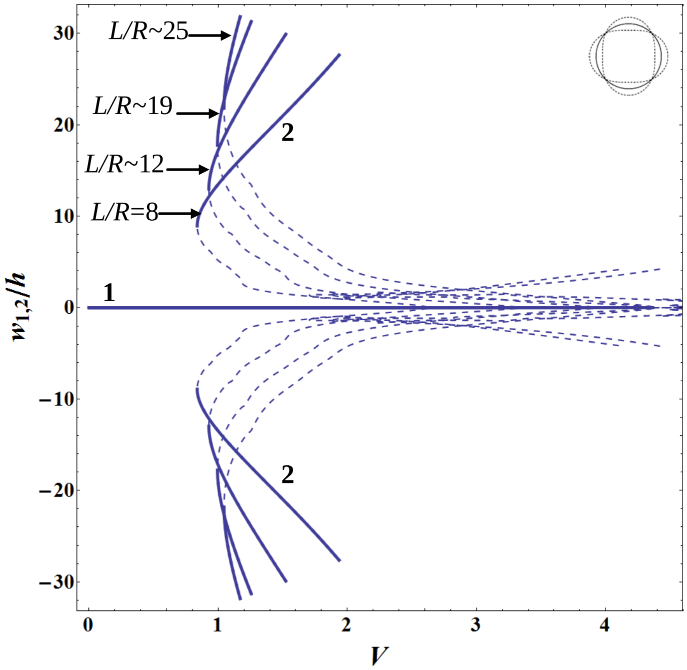

FIGURE 4: Nonlinear bifurcation analysis of the nondimensional blood flow versus the nondimensional aorta radial deformation for different length-to-radius ratios with n=2 for the first asymmetric modes and ΔP_{tm}=0. ———, Stable solutions; – – – –, unstable solutions. **1** and **2** indicate different solution braches.

3.3 Nonlinear response of aorta for different *E* values

The aorta system was tested for different Young's modulus values to determine the effect of stiffness on the stability of the system. In addition, the axial springs were stiffened to model clamped boundary conditions (enabling tension forces at the end of the aortic segment) and the rotational spring was set to zero to allow for radial rotations at the aorta ends. Fig. 5 shows a comparison of aortas with L/R=8 and n=2 for different values of E [32]. For the single-layered shell model the effect of E on the stability of the system was investigated by choosing the following values: 100, 400, and 800kPa [42, 43]. The results show that lower E values significantly reduce the critical flow for instability. However, higher E values result in smaller deformation amplitudes once folding occurs. Nevertheless, it is evident that the aorta amplitude is rather large for the cases shown in Fig. 5. In all cases the aorta loses stability by divergence exhibiting strong nonlinear subcritical behaviour.

Additional results for different length-to-radius ratios are shown below in Fig. 6 for a circumferential wavenumber n=3. All systems lose stability by divergence, followed by a strong subcritical behaviour.

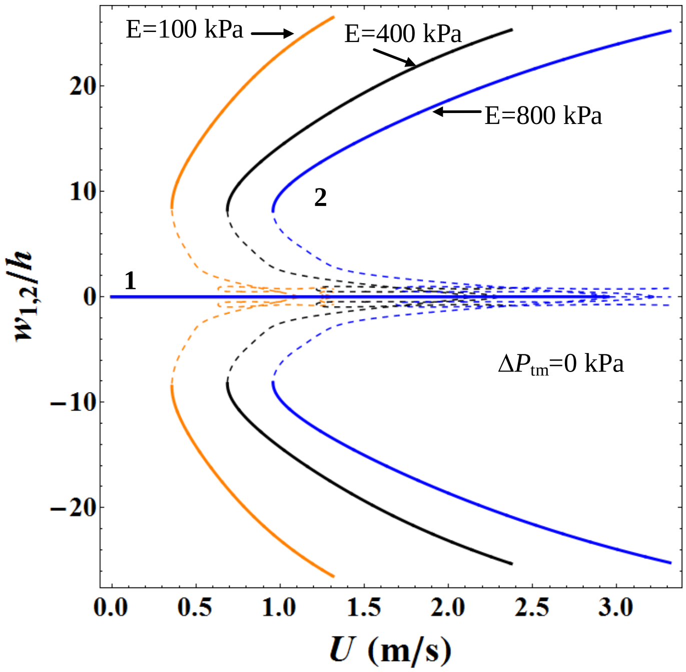

FIGURE 5: Comparison of aorta systems with L/R=8 and different E values for the first asymmetric mode with n=2.

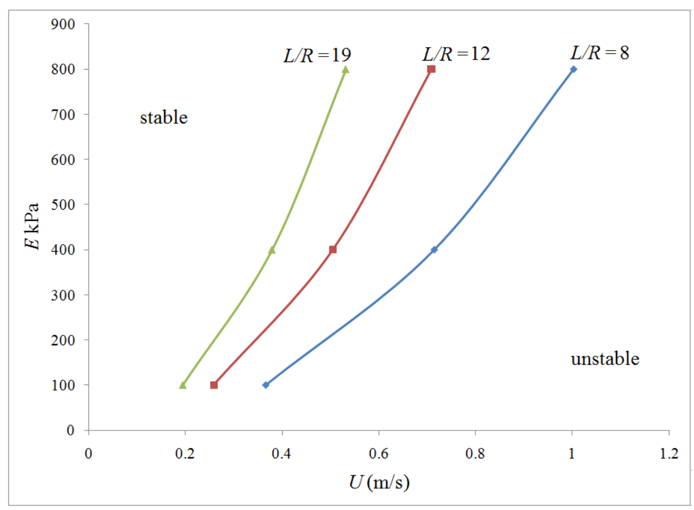

FIGURE 6: Comparison of aorta systems for different L/R ratios and different E values, ΔP_{tm}=0 for the first asymmetric mode with n=3.

3.4 Nonlinear response of aorta for different ΔP_{tm}

Fig. 7 shows a series of comparisons obtained from numerical experiments for different aortas with variable transmural pressurization. Once more the system loses stability by divergence exhibiting strong subcritical behaviour. Evidently, an increase in the transmural pressure value delays the linear onset of instability and produces larger displacements once the solution branch folds and becomes stable again. Therefore, even though pressurizing the aorta seems to delay the instability from occurring at low blood flow velocity values, in reality it yields a highly subcritical system (the range between the linear onset for instability and the re-stabilization flow velocity is larger for higher ΔP_{tm}) with large stable radial deformation after folding. The results in Fig. 7 are for a circumferential wavenumber n=3. Additional results on the effect of the transmural pressure for different E values and n=2 are summarized in Fig. 8 below.

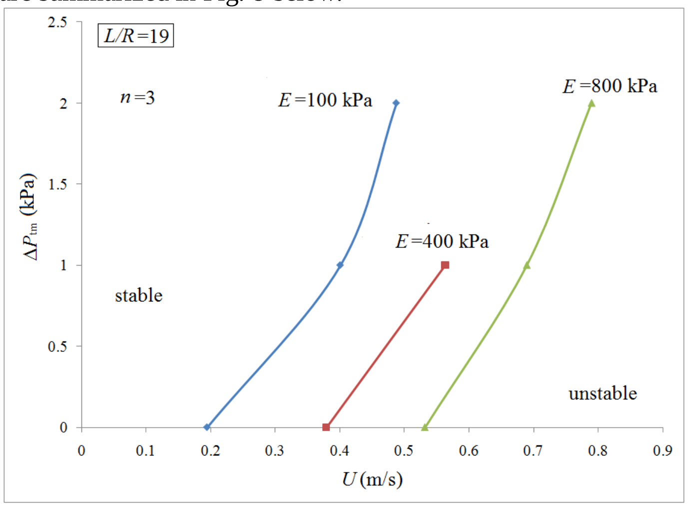

FIGURE 7: Effect of transmural pressure on the subcritical behaviour of aorta conveying blood flow for L/R=19 with h=0.0015 m for the first asymmetric mode with n=3.

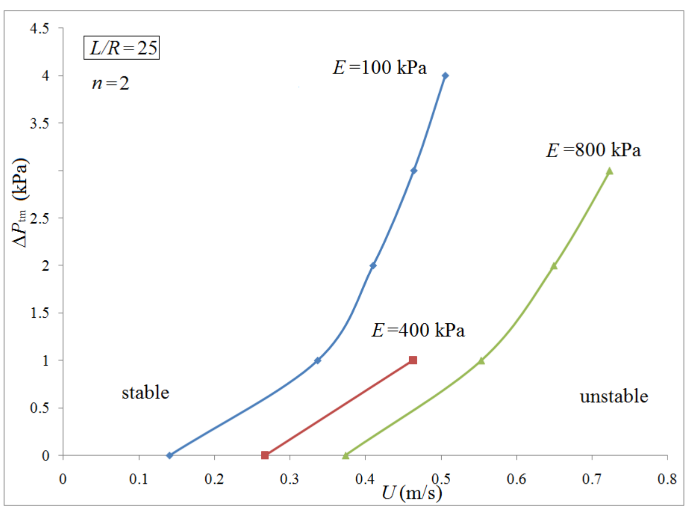

FIGURE 8: Effect of transmural pressure on the subcritical response of an aorta for L/R=25, R/h=10 and n=2.

3.5 Nonlinear response of aorta for different R/h ratios

It is well known that the measured total thickness of the human aorta depends on the individual's health, age, geographical location, and also measurement technique used [22, 44, 45]. A feature of living tissue is its ability to change in size (thickness) with increasing mechanical loading [46]. As expected, the thickness value of the aorta plays an important role in dissection [47]. A typical set of results for different R/h, L/R and E values is shown in Fig. 9. The mean R/h ratio for the human aorta is between 9 and 14; however, there is data available in literature that propose much higher ratios: 20 to 25. Thinning of the aorta due to age, pathological (aneurysm, Marfan disease, diffuse cystic medionecrosis for example) and genetic reasons has been recorded in literature [48].

The results indicate that all systems lose stability by divergence following a subcritical response. The thinner aorta restabilizes at much lower flow velocities, and in the shorter aorta case *islands* of stable solutions are produced before reaching the folding point velocity. Furthermore, the amplitude of the thinner aorta when the solution of branch 2 is stable is larger than the one predicted for thicker aortas for both L/R ratios. In addition, the point of the linear onset of instability is higher for thinner aortas than for thicker aortas.

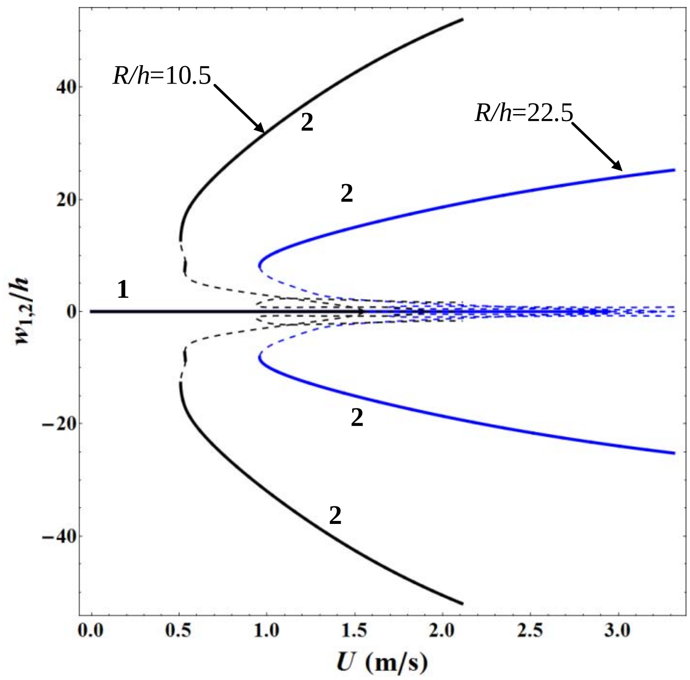

FIGURE 9: Effect of thickness on the aorta response for different L/R ratios and ΔP_{tm}=0 kPa, L/R=8, E=800 kPa and n=2.

4. CONCLUSIONS

A new theoretical framework for the nonlinear fluid-structure interaction of human aortas conveying blood flow is presented in this study. Large arteries like the aorta are continuously subjected to significant mechanical loads from internal blood flow and surrounding tissue and muscle, making them prone to small-scale oscillations and probable wall thinning, which in pathological cases might lead to aorta dissection.

The results showed that flow-induced buckling (or even collapse) of the aorta is possible under specific flow and pressure conditions. Furthermore, the aorta under these critical conditions is characterized by a highly subcritical nonlinear behavior, with multiple stable solutions (zero deformation cylindrical shape, buckled aorta, or total collapse) coexisting for a large range of blood flow velocities. Even partial collapse of the aorta might cause catastrophic failure because it would constrict the blood flow or induce dynamic divergence as observed in experiments [49, 50].

It was found that a longer aortic segment (larger L/R) loses stability at smaller critical flow velocity (linear onset of instability), reduces the natural frequency and increases the subcritical range of flow velocities. A stiffer material delays the onset of instability but, exhibits a similarly strong subcritical response. The effect of reducing the thickness of the aorta is to induce instability earlier and reduce the subcriticality of the system; however, it produces larger aorta deformation. Increasing ΔP_{tm} renders the system more stable with respect to the onset of divergence, and it induces a *ballooning* effect. It is here conjectured that the pressurization-depressurization of the aorta due to systolic-diastolic cycle or a strenuous exercise regime might be responsible for the constant oscillation of the aorta, which coupled with a cardiovascular disease or other pathological problems might induce material deterioration and thus the appearance and growth of aneurysms and dissection.

This study presents for the first time the possibility of subcritical collapse of aortic segments which could be of critical importance in human health. In addition, for the first time, a global analysis tool, namely classical bifurcation analysis has been used to obtain all stable and unstable solutions associated with aortas conveying blood flow, thus allowing for the full set of results for a range of flow velocities to be investigated.

ACKNOWLEDGEMENT

The authors would like to thank the NSERC Discovery Grant program, Canada Research Chair and Canada Foundation for Innovation programs for their financial support, as well as McGill University for a start-up grant.

REFERENCES

[1] Kamm, R.D., Pedley, T.J., 1989. “Flow is collapsible tubes: A brief review”. *Journal of Biomechanical Engineering* **111**, pp. 177-179.

[2] Bertram, C.D., 1995. “The dynamics of collapsible tubes”. *Symposia of the Society for Experimental Biology* **49**, pp. 253-264.

[3] Païdoussis, M.P., 2003. *Fluid-Structure Interactions: Slender Structures and Axial Flow*, Vol. 2. Elsevier Academic Press, London, UK.

[4] Luo, X.Y., Pedley, T.J., 1996. “Flow and instability in collapsible tubes”. *ZAMM Zeitschrift fur Angewandte Mathematik und Mechanik* **76**, pp. 37-40.

[5] Heil, M., 1996. “The stability of cylindrical shells conveying viscous flow”. *Journal of Fluids and Structures* **10**, pp. 173-196.

[6] Heil, M., 1998. “Stokes flow in collapsible tubes – Computation and experiment”. *Journal of Fluid Mechanics* **353**, pp. 285-312.

[7] Keller, J.B., Antman, S., 1969. *Bifurcation theory and nonlinear eigenvalue problems*. W.A. Benjamin, Inc., U.S.A.

[8] Thompson, J.M.T., Stewart, H.B., 1988. *Nonlinear dynamics and chaos*, John Wiley & Sons, Inc., USA.

[9] Amabili, M., Pellicano, F., Païdoussis, M.P., 1999. “Nonlinear dynamics and stability of circular cylindrical shells containing flowing fluid. Part I: Stability”. *Journal of Sound and Vibration* **225**, pp. 655-699.

[10] Amabili, M., Pellicano, F., Païdoussis, M.P., 1999. “Nonlinear dynamics and stability of circular cylindrical shells containing flowing fluid. Part II: large-amplitude vibrations without flow”. *Journal of Sound and Vibration* **228**, pp. 1103-1124.

[11] Amabili, M., Pellicano, F., Païdoussis, M.P., 2000. “Nonlinear dynamics and stability of circular cylindrical shells containing flowing fluid. Part III: truncation effect without flow and experiments”. *Journal of Sound and Vibration* **237**, pp. 617-640.

[12] Amabili, M., Pellicano, F., Païdoussis, M.P., 2000. “Nonlinear dynamics and stability of circular cylindrical shells containing flowing fluid. Part IV: large-amplitude vibrations with flow”. *Journal of Sound and Vibration* **237**, pp. 641-666.

[13] Karagiozis, K.N., Païdoussis, M.P., Amabili, M., Misra, A.K., 2008. “Nonlinear stability of cylindrical shells subjected to axial flow: Theory and experiments”. *Journal of Sound and Vibration* **309**, pp. 637-676.

[14] Barabas, M., Gosselin, G., Crépeau, J., Petitclerc, R., Cartier, R., Théroux, P., 2000. “Left main stenting-as a bridge to surgery- for acute type A aortic dissection and anterior myocardial infarction”. *Catheterization and Cardiovascular Intervention* **51**, pp. 74-77.

[15] Xavier, R., Bourdeaud’Hui, A., Collet, D., Laborde, N., Baudet, E., 1989. “Traumatic rupture and aneurysm of the aortic isthmus: Late results of repair by direct suture”. *Annals of Vascular Surgery* **3**, pp. 47-51.

[16] Khanafer, K., Berguer, R., 2009. “Fluid-structure interaction analysis of turbulent pulsatile flow within a layered aortic wall as related to aortic dissection”. *Doi:10.1016/j.jbiomech.2009.08.010*.

[17] Wang, D.S., Dake, M.D., 2006. “Endovascular therapy for aortic dissection”. In: Rousseau, H., Verhoye, J.P., Heautot, J.F. (Eds.), *Thoracic Aortic Diseases*. Springer, New York, NY, pp. 189-198.

[18] Chavanon., O., Carrier, M., Cartier, R., Hébert, Y., Pellerin, M., Pagé, P., Perrault, L.P., 2001. “Increased incidence of acute ascending aortic dissection with off-pump aortocoronary bypass surgery”. *Annals of Thoracic Surgery* **71**,

117-121.

[19] Gao, F., Watanabe, M., Matsuazawa, T., 2006. "Stress analysis in a layered aortic arch model under pulsatile blood flow". *BioMedical Engineering Online* **5**, art. 25.

[20] Pemberton, J., Sahn, D.J., 2004. "Imaging of the aorta". *International Journal of Cardiology* **97**, pp. 53-60.

[21] Heil, M., Pedley, T.J., 1996. "Large post-buckling deformations of cylindrical shells conveying viscous flow". *Journal of Fluids and Structures* **10**, pp. 565-599.

[22] Tremblay, D., Zigras, T., Cartier, R., Leduc, L., Butany, J., Mongrain, R., Leask, R.L., 2009. "A comparison of mechanical properties of materials used in aortic arch reconstruction". *The Annals of Thoracic Surgery* **88**, pp. 1484-1491.

[23] Amabili, M., Karagiozis, K., Païdoussis, M.P., 2009. "Effect of geometric imperfections on nonlinear stability of circular cylindrical shells conveying fluid". *International Journal of Non-Linear Mechanics* **44**, pp. 276-289.

[24] Amabili, M., 2008. *Nonlinear Vibrations and Stability of Shells and Plates*. Cambridge University Press, New York, USA.

[25] Selmane, A., Lakis, A.A., 1997. "Non-linear dynamic analysis of orthotropic open cylindrical shells subjected to a flowing fluid". *Journal of Sound and Vibration* **202**, pp. 67-93.

[26] Païdoussis, M.P., Denise, J.P., 1972. "Flutter of thin cylindrical shells conveying fluid". *Journal of Sound and Vibration* **20**, pp. 9–26.

[27] Païdoussis, M.P., Misra, A.K., Chan, S.P., 1985. "Dynamics and stability of coaxial cylindrical shells conveying viscous fluid". *Journal of Applied Mechanics* **52**, pp. 389-396.

[28] Doedel, E.J., Champneys, A.R., Fairgrieve, T.F., Kuznetsov, Y.A., Sandstede, B.., Wang, X., 1998. *AUTO 97: Continuation and Bifurcation Software for Ordinary Differential Equations (with HomCont)*, Concordia University, Montreal, Canada.

[29] Dobrin, P.B., 1978. "Mechanical properties of arteries". *Physiological Reviews* **58**, pp. 397-460.

[30] Li, A.E., Kamel, I., Rando, F., Anderson, M., Kumbasar, B., Liam, J.A.C., Bluemke, D.A, 2004. "Using MRI to access aortic wall thickness in the multiethnic study of atherosclerosis: Distribution by race, sex and age". *American Journal of Roentgenology* **182**, pp. 593-597.

[31] Labrosse, M.R., Beller, C.J., Mesana, T., Veinot, J.P., 2009. "Mechanical behaviour of human aortas: Experiments, material constants and 3-D finite element modeling including residual stress". *Journal of Biomechanics* **42**, pp. 996-1004.

[32] Gao, F., Guo, Z., Sakamoto, M., Matsuzawa, T., 2006. "Fluid-structure interaction within a layered aortic arch model". *Journal of Biological Physics* **32**, pp. 435-454.

[33] Johnston, B.M, Johnston, P.R., Corney, S., Kilpatrick, D., 2004. "Non-Newtonian blood flow in human right coronary arteries: steady state simulations". *Journal of Biomechanics* **37**, pp. 709-720.

[34] Johnston, B.M, Johnston, P.R., Corney, S., Kilpatrick, D., 2006. "Non-Newtonian blood flow in human right coronary arteries: Transient simulations". *Journal of Biomechanics* **39**, pp. 1116-1128.

[35] Farcas, M.A., Rouleau, L., Fraser, R., Leask, R.L., 2009. "The development of 3-D, in vitro, endothelial culture models for the study of coronary artery disease". *Biomedical Engineering Online* **8**, art. 30.

[36] Liu, S.Q., Yen, M., Fung, Y.C., 1994. "On measuring the third dimension of cultured endothelial cells in shear flow". *Proceedings of the National Academy of the United States of America* **91**, pp. 8782-8786.

[37] Mills, C., Gabe, I., Gault, J., Mason, D., Ross, J., Braumwald, E., Shillingford, J., 1970. "Pressure-flow relationships and vascular impedance in man". *Cardiovascular Research* **4**, pp. 405-417.

[38] Weaver, D.S., Unny, T.E., 1973. "On the dynamic stability of fluid-conveying pipes". *Journal of Applied Mechanics* **40**, pp. 48-52.

[39] Volokh, K.Y., Vorp, D.A., 2008. "A model of growth and rupture of abdominal aortic aneurysm". *Journal of Biomechanics* **41**, pp. 1015-1021.

[40] Novelline, R.A., Rhea, J.T., Rao, P.M., Stuk, J.L., 1999. "Helical CT in emergency radiology". *Radiology* **213**, pp. 321-339.

[41] Holzapfel, G.A., Sommer, G., Regitnig, P., 2004. "Anisotropic mechanical properties of tissue components in human atherosclerotic plaques". J*ounal of Biomechanical Engineering* **126**, pp. 657-665.

[42] Lang, R.M., Cholley, B.P., Korcarz, C., Marcus, R.H., Shroff, S.G., 1994. "Measurement of regional elastic properties of the human aorta. A new application of transesophageal echocardiography with automated border detection and calibrated subclavian pulse tracings". *Circulation* **90**, pp. 1875-1882.

[43] Wuyst., F.L., Vanhuyse, V.J., Langewouters, G.J., Decraemer, W.F., Raman, E.R., Buyle, S., 1995. "Elastic properties of human aortas in relation to age and atherosclerosis: a structural model". *Physics in Medicine and Biology* **40**, pp. 1577-1597.

[44] Choudury, N., Bouchot, O., Rouleau, L., Tremblay, D., Cartier, R., Mongrain, R., Leask, R.L., 2009. "Local mechanical and structural poperties of healthy and diseased human ascending aorta tissue". *Cardiovascular Pathology* **18**, pp. 83-91.

[45] Langewouters, G.J., Wesseling, K.H., Goedhard, W.J.A.,

1984. “The static elastic properties of 45 human thoracic and 20 abdominal aortas *in vitro* and the parameters of a new model”. *Journal of Biomechanics* **17**, pp. 425-435.

[46] Rachev, A., Stergiopulos, N., Meister, J.-J., 1996. “Theoretical study of dynamics of arterial wall remodeling in response to changes in blood pressure”. *Journal of Biomechanics* **29**, pp. 635-642.

[47] Yee, C.A., 2004. “Aortic dissection: the tear that kills”. *Nursing Management* **35**, pp. 25-32.

[48] Hayes, J.A., Woo-Ming, M.O., 1965. “Diffuse cystic medionecrosis and aortic thinning”. *Dis Chest* **48**, pp. 645-648.

[49] Karagiozis, K.N., Païdoussis, M.P., Misra, A.K., Grinevich, E., 2005. “An experimental study of the nonlinear dynamics of cylindrical shells with clamped ends subjected to axial flow”. *Journal of Fluids and Structures* **20**, pp. 801-816.

[50] Karagiozis, K.N., 2006. *Experiments and theory on the nonlinear dynamics and stability of clamped shells subjected to axial fluid flow or harmonic excitation*. PhD thesis, McGill University, Montreal, Canada.

